Changes in Injection Well Capacity During Testing and Plant Start-Up at Ngatamariki

Jonathon Clearwater, Lutfhie Azwar, Mike Barnes, Irene Wallis and Robert Holt
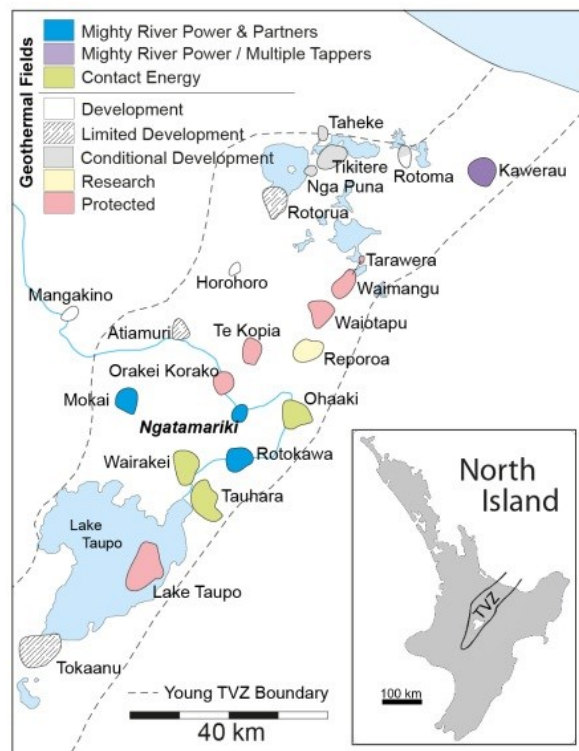
Jonathon.Clearwater@mightyriver.co.nz

ABSTRACT

The Ngatamariki geothermal field is situated 17 km north east of Taupo, New Zealand, and in 2013 Mighty River Power commissioned an 82 MW power station on the field consisting of four Ormat Energy Converter units. Production is from three deep wells in the center of the field and injection is back into four deep wells split between the North and South. Four of these wells were drilled during a campaign in 2012, including three injection wells. In addition to the normal completion testing, each of the new injection wells was injected with cold river water for several weeks to determine potential for stimulation. Prior to plant start-up, proved injection capacity was less than 50% of what was required to run the plant at full generation. Data from the stimulation testing phase constrained a simple analytic model of well stimulation based on Grant et al. (2013) and this model was used to predict injectivity evolution during plant start-up. Modeling predicted the injection wells would stimulate up to the required capacity during the staged start-up of the four Ormat units with minimal generation losses, and accordingly the decision to drill an additional injection well was deferred. During plant start-up the injection wells did stimulate within the predicted range. This paper presents the injectivity index data during injection stimulation testing with cold river water and during plant operation when the wells were injected with 90°C geothermal brine. The injectivity evolution is discussed in the context of the geological structure and fracture properties of the rocks, micro-seismic activity and recent developments in well stimulation modeling.
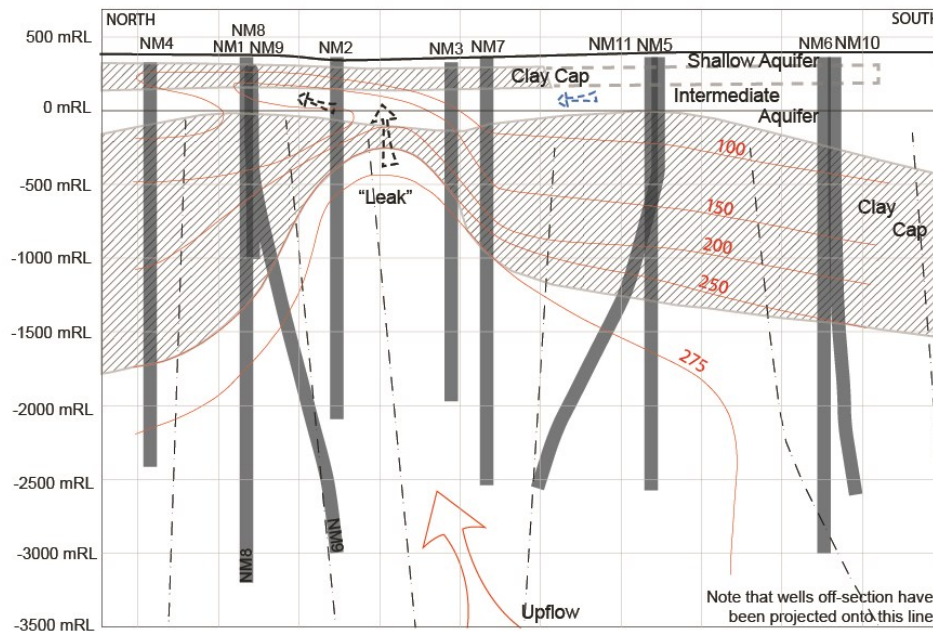
1. INTRODUCTION

The Ngatamariki geothermal field is located 17 km north-east of Taupo in the Taupo Volcanic Zone as show in Figure 1. It is one of a number of high-temperature geothermal systems which lie within an active volcano-tectonic depression (the Taupo Volcanic Zone) formed within a Mesozoic meta-sedimentary basement (Wilson et al., 1995). During a campaign, started in 1984 by the New Zealand (NZ) government, four deep wells were drilled in the reservoir indicating a potential resource for development. However, an NZ-wide lack of interest in geothermal during the 1990's meant further drilling would wait until 2004 when Mighty River Power (MRP) partnered with Tauhara North #2 Trust to drill three very promising wells into the deep reservoir. Following this drilling, an updated MT survey, and intensive feasibility and modeling studies (Boseley et al, 2010; Clearwater et al, 2011), a decision was made to proceed with staged development of an 82MW power station.

Figure 1: Location of Ngatamariki and other high-temperature geothermal fields in the Taupo Volcanic Zone (TVZ), New Zealand. Field boundaries are as given by Bibby et al. (1995) and the boundary of the Young TVZ is by Wilson et al. (1995).

A key feature of the Ngatamariki reservoir is the presence of a cool "intermediate aquifer" sitting above the deep reservoir and the localized permeability pathway between them known as "the leak" (see Figure 2). Because of this leak structure, the risk of cold water downflow as a consequence of pressure drawdown in the main reservoir was identified as an important development risk. Subsequently it was decided to proceed with a 100% injection strategy and use Ormat technology for the power plant. To support the mass flow requirements for the new plant a drilling campaign was initiated in late 2011 for three new injection wells and one new production well. The development strategy was to inject in the north and south of the field while producing from the center to maintain maximum flexibility in shifting injection for optimal reservoir management.

Figure 2: Basic conceptual model of the Ngatamariki reservoir. Cross-section is approximately 5.5 km long (adapted from Boseley et al, 2011).

Injection wells in other MRP fields have responded positively when injected with cooler fluid (Grant et al, 2013). Accordingly, in addition to standard completion testing, each injection well was injected with cold river water while monitoring the well's injectivity index to assess the potential for stimulation. Electric wire line logs, both petrophysical and image-type, were acquired in selected well intervals to characterize the rock mechanical and fracture properties. Stress orientation and magnitude was constrained utilizing log data and extended leak-off testing conducted at each casing shoe (note $S_v > S_{Hmax} > S_{hmin}$). Micro-seismic data was recorded throughout the drilling, testing and development phases. Together these data have enabled us to explore the mechanisms of thermal stimulation in Ngatamariki wells with the goal of constructing predictive models of well stimulation. The three injection wells did stimulate with cold water injection below the fracture gradient (S_{hmin}); however, prior to plant startup, total injection capacity was less than half of what was required to run the power plant at full capacity. The four 20.5 net MW Ormat Energy Converter (OEC) units were planned to be commissioned with several-week gaps between each unit, which, according to a simple analytic model of well stimulation, allowed for the wells to stimulate up just in time to allow each new unit to be brought on with minimal constraints. A key uncertainty when extrapolating stimulation testing results into development was that the testing fluid was 10 °C to 20 °C pure river water while during development wells would be injected with 90 °C geothermal brine. At that time it was not clear what impact the different water temperature would have although the different chemistry of the injection brine was not expected to be a concern.

In this paper we present the injectivity index (*II*) data during well stimulation testing and plant start-up, noting that all testing and well operation was conducted well below the fracture gradient. We explore the mechanisms of existing permeability and reasons for permeability enhancement utilizing a robust suite of reservoir data. Results are discussed with regard to several new developments in well stimulation modeling (Dempsey et al, 2013; Grant et al, 2013).

2. INJECTIVITY INDEX DURING WELL STIMULATION PHASE

In a review of MRP injection well stimulation Grant et al (2013) found that many wells show an *II* improvement over time that follows a power law with an exponent between 0.3 and 0.7. That is, the *II* tended to follow a relationship like

$$II = Ct^n \tag{Eq. 1}$$

where *C* is a constant, *t* is time since stimulation began and *n* is the power law exponent with a value between 0.3 and 0.7. When plotted in log-log space, a linear fit to the data yields a straight line with a slope of *n*. In this paper the value of *n* is referred to as the *stimulation slope* as it is a useful measure to characterize and predict the stimulation performance of injection wells. A simplified theory is developed in Grant et al (2013) discussing a potential physical process underlying Equation 1.

NM08

NM08 is a large diameter, deep, edge-field injection well on the northern margin of the Ngatamariki geothermal field, completed 16th May 2012 to a depth of 3600 mVD. Although NM08 encountered poor permeability it responded very well to cold water

stimulation; the injectivity index improved from 0.4 t/h·bar to 2.7 t/h·bar over 31 days of 10 °C river water injection. The stimulation test data of well-head pressure (WHP) and flow-rate is presented in Figure 3. This data was converted to an injectivity index (II) over time using

$$WHP = P_r - \rho g Z + \frac{W}{II} + KW^2$$

where P_r denotes reservoir pressure, ρ is density, g is gravity, Z is vertical distance down the well, W is mass flow rate, and K is a coefficient to account for frictional forces that was set to zero (friction ignored) to get consistent results with wellbore modeling.
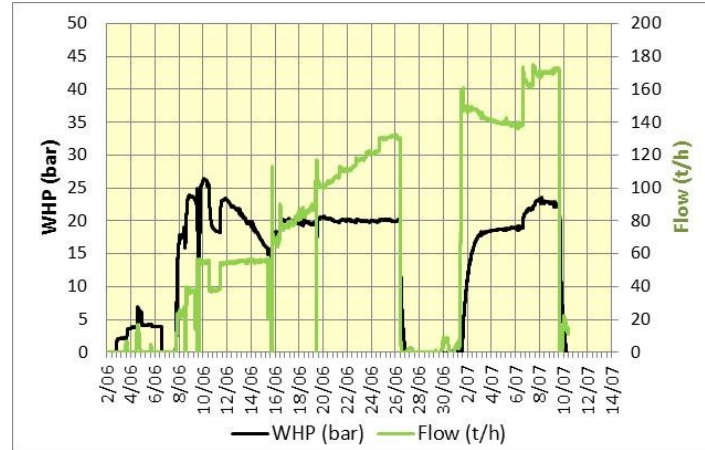

Figure 3: NM08 well-head pressure (WHP) and flowrate during the stimulation test

Plotting the II over time on a log-log plot (taking day one as the first day of injection) and fitting a straight line to the data in log-log space gives a line with stimulation slope of 0.7, as shown in Figure 4. This data was also analyzed in a coupled thermal-hydrological-mechanical model by Dempsey et al (2013) who suggested that the high stimulation slope was associated with a planar stimulated zone geometry.
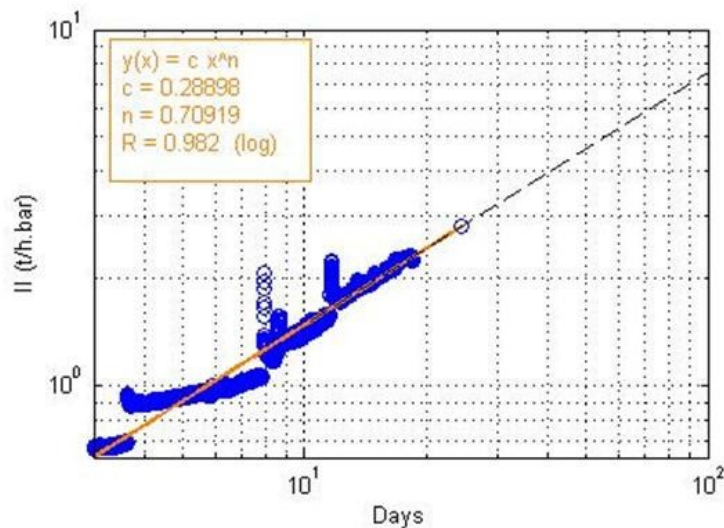

Figure 4: NM08 Injectivity index (II) over time during stimulation period on log-log plot

NM09

NM09 was also drilled as a large diameter, deep edge-field injection well in the north of the Ngatamariki geothermal field on the same drilling pad as NM08, but deviated southeast. After drilling to completion depth 3551mVD on 6 November 2012 the well was estimated to be accepting 144 t/h with no wellhead pressure, indicating a minimum II of 3.5 t/h·bar. This was not confirmed with a proper completion test and the well was left shut-in from 10 October 2012 until the stimulation test began on 14 December 2013. At the beginning of the stimulation test, while injecting at 130t/h the well had a WHP of 1.5bar gauge, indicating the well had lost some injectivity while shut in. NM09 responded positively to cold water stimulation as can be seen in the decreasing downhole pressure (DHP) during relatively constant injection flows shown in Figure 5.
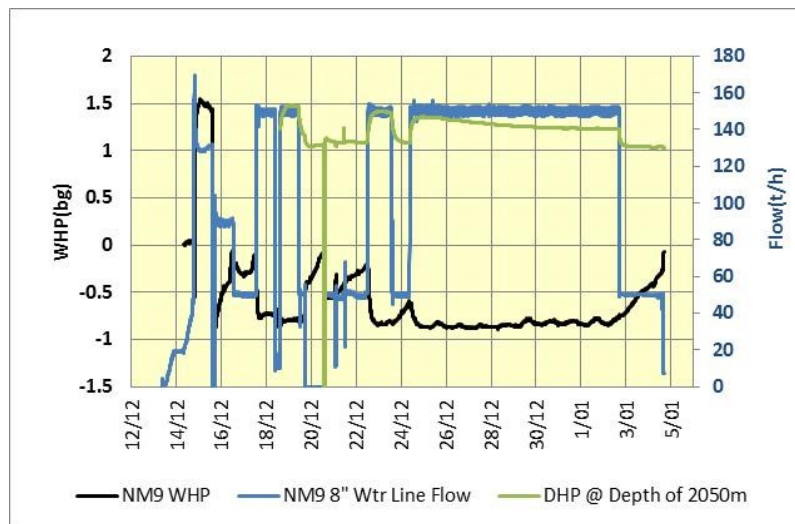
Clearwater et al.

Figure 5: WHP, flow and downhole pressure (DHP) for NM09 during stimulation testing

By 2 January 2013, after 19 days stimulation, NM09 had an *II* of 8.1 t/h·bar. The *II* was calculated by taking the clean data between 24 December 2012 and 3 January 2013, assuming day one as start of the completion test on 14 December 2012, correcting the downhole pressure for nitrogen and adjusting it to an equivalent pressure at the 2400m (pivot) and then calculating $II = \frac{W}{P_{well} - P_{res}}$. Plotting the *II* over time as per Figure 6 gives a straight line fit in log-log space with a stimulation slope of 0.6. This represents very reasonable stimulation, but note there is a change in slope in the data on about day 15 of stimulation. This is unusual because typically wells follow a straight line on a log-log plot and it's not clear what causes this reduction in stimulation rate. Fitting a log-log straight line to the data after day 15 gives a slope of 0.4, so we recognized some uncertainty as to the appropriate slope for predicting further stimulation, using a range of 0.4 to 0.6.
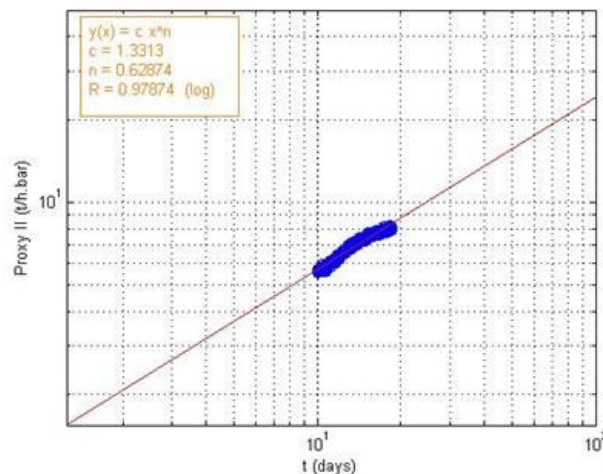

Figure 6: NM09 II over time during stimulation test on loglog plot

NM10

NM10 was drilled as a deep edge-field injection well in the south of the Ngatamariki geothermal field. NM10 is a standard sized bore completed with 7" perforated liner to a total drilled depth of 3035mRT (2833.97mTVD from ground surface), and was drilled between May and August 2012. The completion test confirmed an *II* of 6.9 t/h·bar. NM10 responded positively to cold water injection and improved to an *II* of 8.9 t/h by the end of the cold river water stimulation test. DHP and flow rate data is presented in Figure 7.
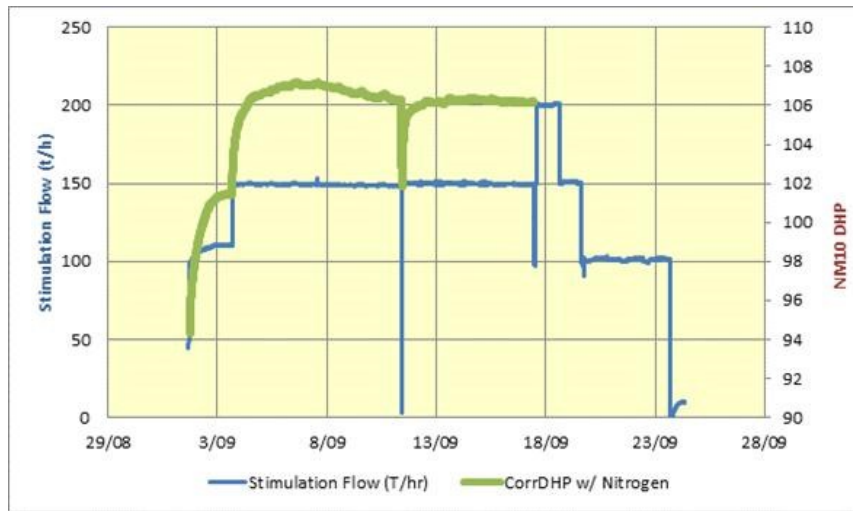
4

Figure 7: DHP and flow rate data for NM10 during stimulation test

To determine a stimulation slope (*n*) the *II* was calculated during the completion test at the beginning of the stimulation phase and also at the three rate test at the end of the stimulation. These two points represented the most accurate *II* data, and the ongoing pressure data was not used because it showed some transient behavior that confounded *II* interpretation. NM10 took full losses early in drilling and cold water was also injected into the well for several weeks due to major rig down-time during drilling, further complicated the analysis because the date of stimulation onset was not clear. The stimulation slope calculated depends on when stimulation is assumed to begin and how the well is assumed to respond during standing. To treat the NM10 scenario, stimulation was assumed to begin on the first day of total losses during drilling and the number of days of stimulation was taken as the number of cumulative days the well was accepting fluid (i.e. periods when the well was left standing are ignored). In this manner the start of the stimulation test is actually day 18 of stimulation (reflecting the stimulation that is hypothesized to occur during the 17 days of losses during drilling), and the end of the test is day 37. Given this treatment, a stimulation slope of 0.35 was calculated as shown in Figure 8.
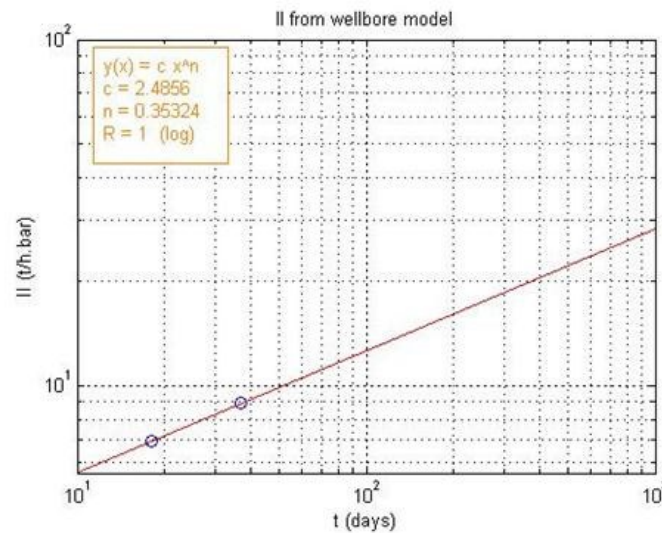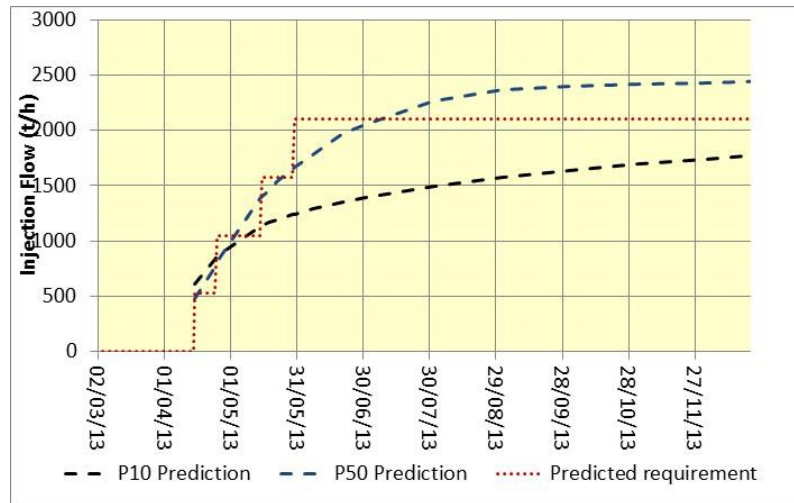

Figure 8: NM10 *II* over time during stimulation test on log-log plot

3. PREDICTING INJECTION CAPACITY DURING PLANT STARTUP

When it came time to commission the first OEC unit, the confirmed injection capacity of the four injection wells was less than half of the requirement for the full 82MW plant operation. It was at this stage that the data obtained during stimulation testing became extremely valuable. Knowing that each of the new wells showed propensity to stimulate with cold water, we developed a simple methodology to predict future injection capacities. The stimulation of each well during testing showed that each well had stimulation consistent with Equation 1, with a range of stimulation slopes from 0.35 to 0.7. A pre-existing injection well, NM06, was also to be utilized; however we had no stimulation-rate information for this well, so it was assumed that NM06 was capable of the injection from a test several years before the start-up.

Extrapolation from the stimulation test data to predict *II* evolution during plant operation was challenging because there were key differences in the temperature and chemical composition of the injected fluid (geothermal brine vs. river water) in the testing and operation phase. The smaller temperature difference between injectate and reservoir fluid in the operational phase was predicted to reduce the stimulation, while the chemical impact of brine vs. river water was predicted to have no effect or to possibly counteract
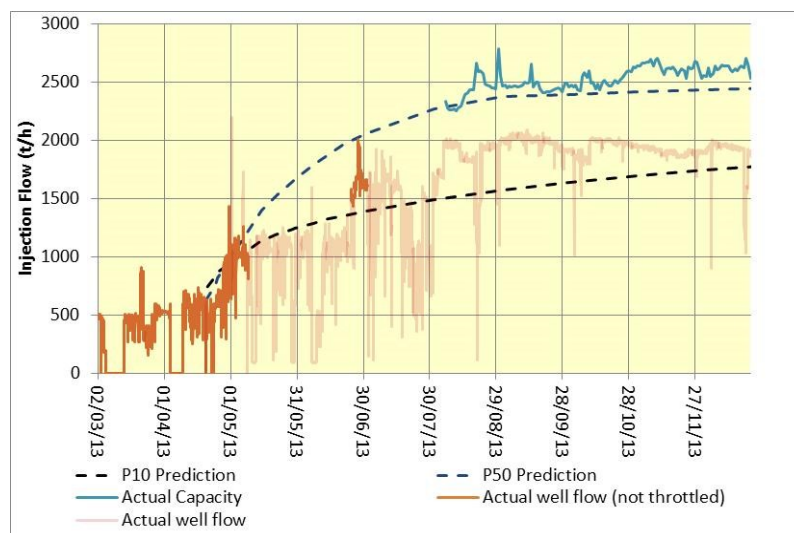
5

thermal stimulation due to precipitation and deposition of scale. Because we did not have a sound theoretical model to account for the chemical processes in predicting well stimulation, and because other fields indicated similar slope range from binary plant injection fluid, we took a pragmatic and conservative approach. We assumed a distribution of stimulation slopes with a P10 value of 0.2 and P50 value of 0.4. This represented our confidence that there was a 90% chance of getting stimulation at least as good as 0.2 and a 50% chance of getting stimulation at least as good as 0.4. For each well Equation 1 was fitted using the particular stimulation slope *n*, and then *C* was adjusted to match a measured *II* on about day 10 of the stimulation test. The predicted *II* was then used to calculate an injection well capacity at operating wellhead conditions. The capacity of each well was summed to give the total predicted injection capacity shown in Figure 9.

Figure 9: The situation prior to plant startup showing total predicted P10 and P50 injection capacities, with injection requirements according to the proposed startup schedule shown in red.

Based on the predictions in Figure 9 the decision was made to defer drilling an additional injection well and to attempt to run the field with the four existing injection wells plus the temporary use of NM03 during the predicted period of injection capacity shortfall to minimize generation losses. This of course saved the significant expenditure of a new well, but ran the risk of severe revenue loss if plant operations were constrained by injection not stimulating as predicted.

The wells did stimulate and the predictions were very reasonable when compared with actual capacities during plant operation. In Figure 10 the dark orange line shows the actual injection well flow when the wells were not throttled, and the solid blue line shows calculated capacity using a wellbore model to infer actual capacity. The data at the end of June 2013 shows a total injection capacity between the P10 and P50 predictions, but by August 2013 the P50 prediction is a close match to the actual capacity. It is worth noting here that during the first few months the quantity and temperature of the injection flows varied considerably due to testing and operational procedures associated with running a new power plant (light orange line in Figure 10). During start-up, injection brine was often greater than 150 °C as production exceeded the plant intake capability and had to be bypassed into the injection system.
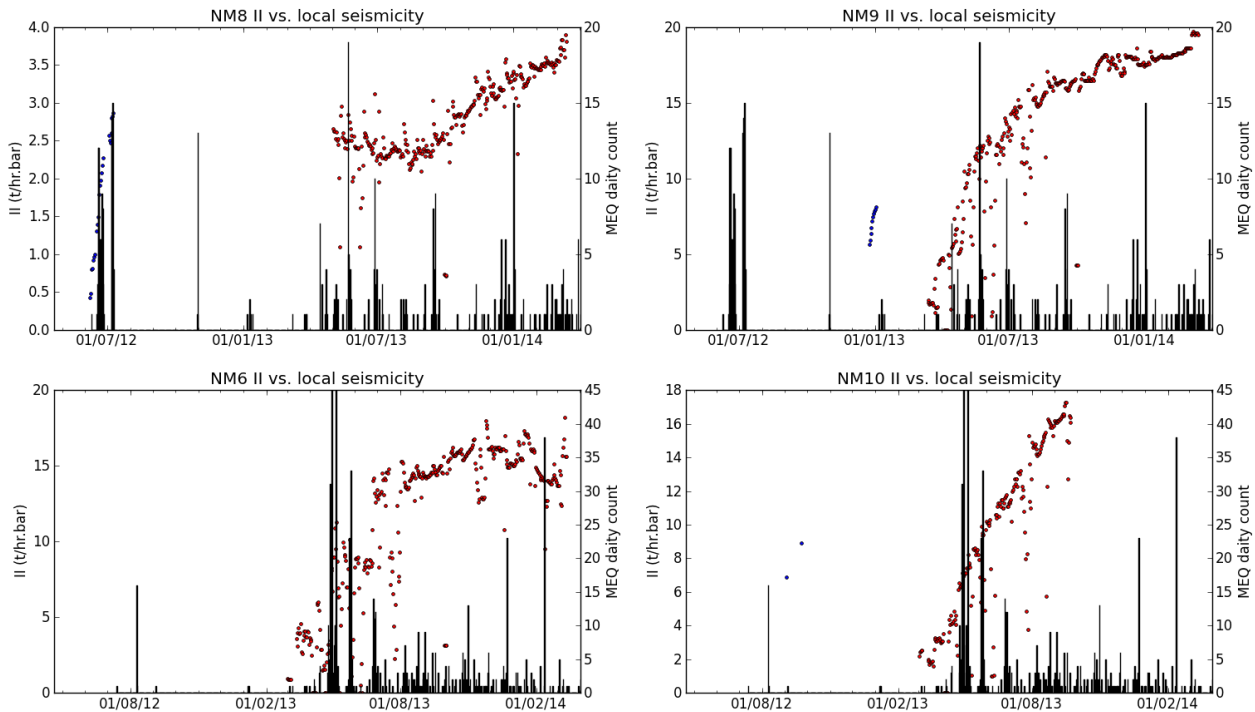

Figure 10: Actual injection capacities during plant startup and operation. The original P10 and P50 predicted capacities are shown in dashed lines. The dark orange line indicates total well flow at operating conditions and the light orange line indicates flow while throttled. The light blue line indicates the calculated actual capacity from wellbore modeling.

4. WELL STIMULATION COMPARISON WITH MICROSEISMIC ACTIVITY

The Ngatamariki seismic network was installed before plant startup in order to provide context for later results. The final seismic network consisted of thirteen stations and the data is augmented by one station within GeoNet's national network. At the time of the stimulation tests, not all stations were installed, but there were enough to detect and locate micro-earthquakes (MEQ) in the region to an acceptable accuracy. It is often observed that increased MEQ activity coincides with significant events e.g. plant shuts or shifts in injection. However, not every plant shut coincides with increased MEQ and increased MEQ will often occur independently of any action at the plant. MEQ represent the release of stress accumulated on a fault and this stress can only be released under favorable conditions of stress magnitude/orientation, pore-fluid pressure and friction. However, if insufficient stress has accumulated on the fault, there may be no release of energy.
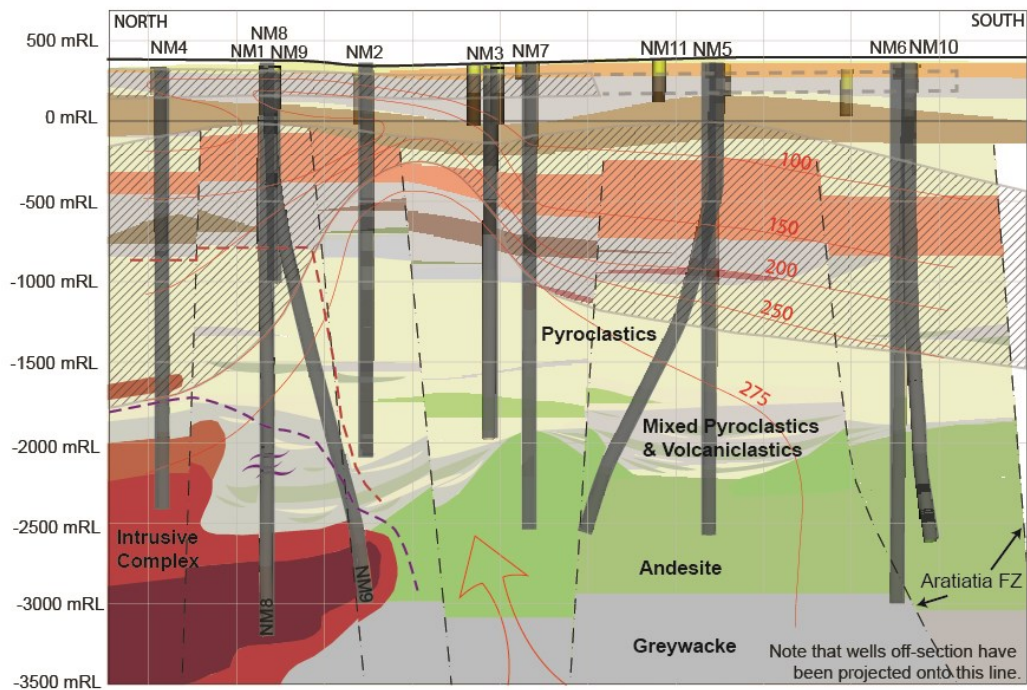
Comparing MEQ and *II* data for stimulation tests and plant start-up, as shown in Figure 11, suggests that the first test at NM08 released accumulated stress. The subsequent test at NM09 coincides with a small number of events and the NM10 test has no corresponding events. Plant start-up appears to have introduced a significant change in earthquake parameters, resulting in a sustained period of elevated seismicity until October 2013, after which seismic activity has settled to background activation levels.

Figure 11: *II* and local MEQ daily counts for each well. Note that the testing phase *II* are shown in blue and *II* during plant operation are shown in red.

5. COMPARISON OF GEOLOGICAL SETTING BETWEEN WELLS

Permeability in a geothermal system is a dynamic relationship involving mechanical (including thermal) and chemical processes (both precipitation and dissolution), governed by the nature of the rocks and those fluids interacting with them. Because development changes the pressure, temperature and chemistry of the fluid circulating in the reservoir, it heightens the potential for both permeability enhancement and destruction. The materials which dominate the subsurface at Ngatamariki (welded pyroclastics, volcaniclastics, andesite lavas and greywacke which have what is, in many cases, extensive alteration overprinting) are typical of the Taupo Volcanic Zone aside from one – a large pluton at depth in the north of the field (Figure 12). The intrusion of this pluton can be thought of as several cross-cutting solid masses of crystalline rock, each encircled by a damage zone and with a magmatic-hydrothermal alteration halo (Lewis et al. 2013) which has had a significant impact on the existing material properties. The presence of this pluton in the north of the field has created a split between the northern and southern injections as to mechanisms for initial rock permeability and well response to stimulation.

Figure 12 Cross-section through the Ngatamariki geologic model with conceptual elements from Figure 2 overlaid. Refer to Chambefort et al. (2014) for a full discussion of stratigraphic elements. The red dashed line indicates the outer extent of phyllic alteration (magmatic-hydrothermal alteration) and the purple dashed lines marks the approximate limit of very intense alteration associated with the intrusive body (magnate limit Lewis et al., 2014).

Permeable zones in the southern injectors (NM06 and NM10) are variously correlated to a reduction in the number of mineralized fractures (as shown by FMI imaging), increases in porosity within the pyroclastics, and the presence of volcaniclastic material overlying the andesite lava or breccias within that lava. Despite this range of primary host lithologies and overprinting alteration, maintenance and improvement of permeability in this sector of the field is likely to be heavily influenced by stresses associated with the Aratiatia Fault Zone. This fault zone has surface ruptures mapped in the vicinity of NM06 and NM10 which indicate it is a recently reactive structure, and the alignment of numerous high-quality located micro-seismic events has been interpreted as representing one segment of this structure.

The occurrence of permeable zones in the northern injectors is dominantly coincident with damage zones surrounding the different phases of intrusive. The large contrast between the initial permeability in NM08 and NM09 is likely due to the fact that the latter is completed within the pluton itself, whereas the bottom-hole of NM09 appears to have intersected a significant damage zone. Furthermore, shallow permeability in NM09 correlates with a well interval which, based on image log, petrophysics and drilling parameter results, appears to pass through a fault zone - perhaps one which is related to the trace of a surface rupture located by Leonard et al. (2010) between NM08 and NM09. This factor would particularly influence the geomechanical behavior of NM09 during stimulation as the number of pre-existing, well-oriented fractures available for reactivation would be significantly increased. Microseismicity which occurred during the completion of NM08 was extraordinarily restricted to directly adjacent the wellbore track around feed zone depths. NM09 was drilled later in the campaign when other activities were occurring on the field, so the MEQ signal associated with this well is not so clear. However, events occurring during the initial drilling and stimulation of this well were more distributed than NM08. Taking together the MEQ distribution, the relative well permeability between NM08 and NM09, and what we know about the geologic nature of the permeable zones, we can infer that the stimulate-able volume associated with the pluton damage zones is smaller than that which is associated with recently active structures.

6. DISCUSSION ON WELL STIMULATION DURING TESTING VS. OPERATION

The total predicted injection capacity evolution over time did turn out to be very reasonable; however, the procedure for making this prediction was *ad hoc*. We gave the stimulation slope (*n*) a conservative range in order to account for the potentially reduced stimulation during plant operation due to smaller thermal differential and the potential for chemical deposition. After setting the P10 and P50 slopes the *C* parameter from Equation 1 was fitted to ensure that injection capacity matched measured capacity after ten days of stimulation and this was used to project capacity forward. It is interesting then to compare the stimulation in the testing and operational phases. This data is presented in Figure 13 and indicates that NM09 and NM10 behaved similarly in testing and operation while NM08 showed very different behavior. NM06, NM09 and NM10 appear to stimulate right from the onset of plant operations but NM08 *II* shows a flat to decreasing trend for five months before it begins to increase in September 2013.
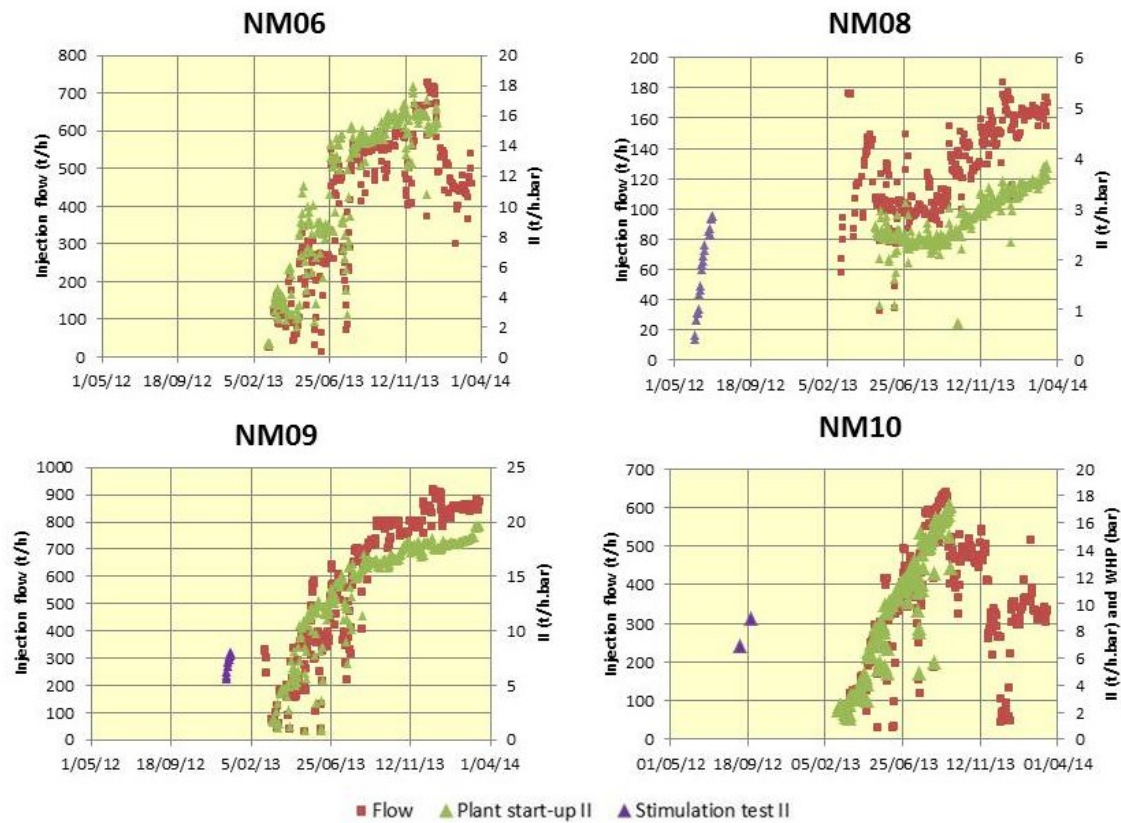
Figure 13: *II* during stimulation test and plant operation

The *C* and *n* values from automatic curve fitting to testing and operational phases are compared in Table 1. In the stimulation test phase the onset of stimulation was assumed to start at the earliest moment the well was accepting continuous cool water into the formation. For NM08 and NM09 this was at the start of the completion test while for NM10 this was the first day of total losses while drilling. In the operational phase the stimulation was assumed to begin on 12 March 2012 as there was reasonably continuous injection after this date.

Table 1: The parameter values for Eq.1 ($II = Ct^n$) during stimulation testing and operation

	Stimulation test		Plant start-up	
	C	*n*	*C*	*n*
NM06			1.06	0.47
NM08[1]	0.29	0.70	0.08	0.66
NM09	1.3	0.62	0.77	0.57
NM10	2.49	0.35	0.50	0.66

In comparing these values we see that all wells decreased the value of *C* when being injected with geothermal brine vs. river water. In NM08 and NM09 the stimulation slope (*n*) was comparable between the stimulation and operating phases, but in NM10 it increased. So it seems that although our approach of reducing the stimulation slope for the operational phase worked to give a reasonable prediction, it may have been more consistent with the data if we had reduced *C* to account for the reduced stimulation under operating conditions.

7. MODELS FOR NM08 BEHAVIOUR

The behavior of NM08 can be split into four distinct phases: *II* improvement during injection with 20°C river water; minimal loss of injectivity while shut in prior to plant start-up; a flat to decreasing *II* trend during five months of brine injection; increasing *II* trend with further brine injection. It is worth noting that the change to an increasing *II* trend with brine injection occurred at

---

[1] For NM08 the II data prior to 1 September 2013 was ignored but the onset of stimulation was assumed to begin on 12/3/2013 to be consistent with the other wells. If we assume stimulation only began on the 1/8/2013, the date at which the II begins to improve, then we get *C = 1.14* and *n = 0.2* for NM08 during operation.

Clearwater et al.

approximately the same time pump rates were increased in NM08 and NM09 to push more injectate to the north of the field. Work is not complete to determine the actual physical processes underlying this behavior, but several working hypotheses are being explored. The most plausible hypotheses are:

1) Competing processes of silica scaling and thermal stimulation

Pure river water poses no threat of silica deposition and as such, during the testing phase, the well exhibited strong thermal stimulation. When initially injected with a low rate of brine into a very large bore, the residence time was just enough to allow the silica to deposit and decrease permeability around the well. With an increase in pump rate the fluid passed into the formation in a shorter time and silica deposition was less likely to occur. Thermal stimulation may have been ongoing, but it was masked during the first five months because of the silica scaling. The finding that the C and n values calculated when stimulation was assumed to begin on the first day of plant operation were more consistent with the behavior in other wells (decreased C and similar n between stimulation and operational phases) is supportive of this hypothesis.

2) New stimulation zone

A rival hypothesis is that the sudden change in II trend was caused by the opening up of a new stimulation zone. This may have been caused by a change in the pressure regime that allowed injection fluid to exit the well at a deeper feedzone and thus allowed stimulation to occur around this new area. It may also be that fluid exiting NM08 followed a pathway such that it encountered an initial fracture network during testing suitable for stimulation (i.e., the damage zones surrounding the different phases of intrusive), but with plant operation it took five months for the fluid to propagate to a new rock volume with a fracture network suitable for stimulation.

Another theory considered the potential for the injection fluid to improve II by dissolving calcite around the wellbore (especially with river water), but this was rejected after geochemical modeling suggested it was not feasible.

8. CONCLUSIONS

This paper narrates how injection well stimulation testing enabled the staged start-up of a geothermal power plant with less than half of the required injection capacity proven. A simple analytic model was developed based on the recognition that injection wells tend to follow a power law improvement in II over time with an exponent between 0.2 and 0.7. This model was calibrated against the stimulation testing data and conservative assumptions were made about how wells would stimulate under plant operation vs. river water injection. Predictions from this simple model in terms of total injection capacity proved to be accurate. This demonstrates the utility of predicting well injection capacity evolution. In this case it allowed the deferral of an additional injection well at a cost saving of several millions of dollars.

This paper also highlights the variety of physical mechanisms of permeability in a geothermal system, mechanical and chemical, and the lack of proper understanding of those physical processes underlying injection well improvement in geothermal. We were not able to predict with higher confidence the performance of the wells during plant operation because we did not know the impact of changing the injectate temperature or chemistry, nor are there clear conceptual models for how the geological setting of each well affects its propensity to stimulate. Some hints at the physical processes underlying the stimulation can be found in the data presented, but there is a need for a more robust model that accurately treats the geomechanics, geochemistry and mass and heat flow with respect to permeability change.

REFERENCES

Bibby, H.M., Caldwell, T.G., Davey, F.J., and Webb, T.H. Geophysical evidence on the structure of the Taupo Volcanic Zone and its hydrothermal circulation: Journal of Volcanology & Geothermal Research, v. 68, p. 29-58 (1995)

Boseley, C., Cumming, W., Urzúa-Monsalve, L., Powell, T., and Grant, M. A Resource Conceptual Model for the Ngatamariki Geothermal Field Based on Recent Exploration Well Drilling and 3D MT Resistivity Imaging *Proceedings World Geothermal Congress* (2012)

Clearwater, J., Burnell, J., and Azwar, L. Modelling the Ngatamariki Geothermal System. *Proceedings, 37th Workshop on Geothermal Reservoir Engineering*, Stanford University, Stanford, CA (2012)

Chamberfort, I., Lewis, B., Wilson, C.J.N., Rae, A.J., Boseley, C., Bignall, G., and Ireland, T.R. Stratigraphy of the Ngatamariki Geothermal System: New U-Pb geochronology and its constraints on Taupo Volcanic Zone evolution. *Journal of Volcanology & Geothermal Research* v. 274, p. 51-70. (2014)

Dempsey, D., Clearwater, J., Kelkar, S., and Wallis, I. Validation of a Coupled Thermal-Hydrological-Mechanical Model Through a Comparative Study of Shear Stimulation in Two Geothermal Environments: USA And New Zealand *Proceedings of the 2013 New Zealand Geothermal Workshop,* Rotorua (2013)

Grant, M, A., Clearwater, J., Quinao, J., Bixley, P. F., Le Brun, M. Thermal Stimulation of Geothermal Wells: A Review of Field Data. *Proceedings of the 38th Stanford Geothermal Workshop*. Stanford University, Stanford, CA (2013).

Halwa, L., Wallis, I., Torres Lozada, G., Geological Analysis of the Volcanic Subsurface Using Borehole Resistivity Images in the Ngatamariki Geothermal Field, New Zealand. Proceedings of the 2013 New Zealand Geothermal Workshop, Rotorua (2013)

Lewis, B., Chamberfort, I., Rae, A.J., and Sanders, F., 2013, Geology of Well NM9, Ngatamariki Geothermal Field, GNS Science Consultancy Report 2012/330.

Rowland, J.V. and Sibson, R.H., Structural controls on hydrothermal flow in a segmented rift system, Taupo Volcanic Zone, New Zealand: *Geofluids*, v. 4, p. 259-283 (2004).

Siratovich, P., Davidson, J., Villeneuve, M., Gravley, D.M., Kennedy, B.M., Cole, J., Wyering, L., and Price, L. Physical and Mechanical Properties of the Rotokawa Andesite from Production wells RK 27_L2, RK 28 and RK 30 *Proceedings of the 2012 New Zealand Geothermal Workshop* (2012)

Verma, A., and Pruess, K.: Enhancement of Steam Phase Relative Permeability Due to Phase Transformation Effects in Porous Media, *Proceedings,* 11th Workshop on Geothermal Reservoir Engineering, Stanford University, Stanford, CA (1986).

Wallis, I., McCormick, S., Sewell, S., and Boseley, C., Formation Assessment in Geothermal Using Wireline Tools – Application and Early Results from the Ngatamariki Geothermal Field, New Zealand. *Proceedings of the 2012 New Zealand Geothermal Workshop,* (2012)

Wang, C.T., and Horne, R.N.: Boiling Flow in a Horizontal Fracture, *Geothermics*, **29**, 759-772 (1999)

Wilson, C.J.N., Houghton, B.F., McWIlliams, M.O., Lanphere, M.A., Weaver, S.D. and Briggs, R.M., Volcanic and structural evolution of Taupo Volcanic Zone, New Zealand: a review. *Journal of Volcanology and Geothermal Research* 68:1-28 (1995)

Wyering, L., Villeneuve, M. and Wallis, I. The Effects of Hydrothermal Alteration on Mechanical Rock Properties of the Andesite Breccia and Tahorakuri Formation from the Ngatamariki Geothermal Field, New Zealand and Empirical Relations Between Rock Strength and Physical Properties *Proceedings of the 2012 New Zealand Geothermal Workshop* (2012)